J. Crop Prot. 2023, 12 (1): 1-13

Research Article

Molecular and in silico analysis of the coat protein of hibiscus chlorotic ringspot virus isolates

Nadia Mosharaf[1], Saeid Tabein[1*], Mehdi Mehrabi-Koushki[1], Seyed Ali Hemmati[1] and Abozar Ghorbani[2]

1. Department of Plant Protection, Faculty of Agriculture, Shahid Chamran University of Ahvaz, Ahvaz, Iran.
2. Nuclear Agriculture Research School, Nuclear Science and Technology Research Institute (NSTRI), Karaj, Iran.

Abstract: Hibiscus chlorotic ringspot virus (HCRSV), genus *Betacarmovirus*, family *Tombusviridae*, is a common pathogen of hibiscus plants in tropical and subtropical regions. During 2020-2021, leaf samples of Chinese hibiscus *Hibiscus rosa-sinensis* L. with mottling and chlorotic ring spot symptoms were collected from Ahvaz and Molasani Khuzestan province, southwestern Iran. Total RNA extracted from symptomatic samples was subjected to RT-PCR analysis to amplify the sequence of the coat protein gene (CP) (*p38*) of HCRSV. Complete (1038 bp) and partial (932 bp) *p38* sequences were determined and deposited in the GenBank database. The consensus sequences obtained from CP were compared with those of known isolates using the nBLAST program and phylogenetic analysis. The phylogenetic tree constructed based on the *p38* sequences showed different ancestors for Iranian isolates of HCRSV. Additionally, the isolates studied were grouped into clades regardless of their geographic distribution, suggesting that there is no differentiation of population based on location and that populations are interconnected. Recombination analysis based on *p38* sequences predicted at least two acceptable recombinant isolates, Ahvaz (Iran) and Israel. *In silico* prediction of CP structures of isolates involved in recombination events showed low sequence to structure identity between HCRSV isolates. In addition to reporting two new HCRSV isolates from Iran, our work demonstrated that HCRSV exhibits a high genetic variation through recombination and that the classification criterion could be changed from low nucleotide sequence identity to a higher value, along with the structural analysis of betacarmovirus proteins.

Keywords: HCRSV, Coat protein, Recombination, Tertiary structure

Introduction

Shrubs of the genus *Hibiscus*, family *Malvaceae*, such as Chinese hibiscus *Hibiscus rosa-sinensis* L. with colorful flowers are native to tropical and subtropical areas around the world (Ramos-Gonzalez *et al.*, 2020). Several *H. rosa-sinenis* varieties are grown as ornamental and landscape plants in urban areas of the Khuzestan province in southwestern Iran.

Handling Editor: Masoud Shams-bakhsh

* Corresponding author: s.tabein@scu.ac.ir
Received: 02 October 2022, Accepted: 29 January 2023
Published online: 28 February 2023

[DOR: 20.1001.1.22519041.2023.12.1.1.9]

Hibiscus chlorotic ringspot virus (HCRSV) was first detected in a hibiscus variety imported into the United States from El Salvador (Jones and Behncken, 1980). HCRSV (genus *Betacarmovirus*, subfamily *Procedovirinae*, and family *Tombusviridae*) has an isometric, non-enveloped particle commonly found in hibiscus plants throughout the world (Jones and Behncken, 1980; Adams *et al., 2*016; Ramos-Gonzalez *et al., 2*020). HCRSV symptoms are mainly found on the leaves of infected *H. rosa-sinenis* plants, including mottling, ringspot, and vein banding (Waterworth *et al., 1*976). Infected vegetative propagules and mechanical transmission are common methods of HCRSV transmission, whereas transmission by seed and vector has not yet been reported (Brunt and Spence, 2000; Pourrahim *et al., 2*013). The first molecularly described HCRSV isolates from Iran were reported from Guilan province, which had the highest sequence identity with the isolate from Singapore (Pourrahim *et al., 2*013).

As a betacarmovirus, the icosahedral particles of HCRSV contain a single-stranded positive RNA genomic fragment (~ 3.9 kb) encoding eight putative open reading frames (ORFs). Two ORFs at the 5' end (*p28* and *p81*) form the viral components of the replicase complex. The downstream genes encode the movement protein (*p9*) and the coat protein (CP) (*p38*), which are translated by two subgenomic RNAs (Huang *et al*., 2000; Navarro and Pallás, 2017). The HCRSV CP functions as an RNA silencing suppressor and a trigger of the hypersensitivity response (Meng *et al., 2*006; Iki *et al., 2*017; Adhab *et al., 2*019). The protein encoded by *p23* may be a critical factor in the viral infection cycle, whereas *p8* does not appear to be transcribed (Huang *et al., 2*000). The proteins encoded by *p25* and *p27* share the same carboxyl terminus and are likely involved in the systemic movement and severity of the symptoms, respectively (Zhou *et al., 2*006).

As demonstrated (Cheng and Nagy, 2003), RNA recombination frequently occurs during betacarmovirus replication by template switching of the viral RdRp (Cheng and Nagy, 2003). The impact of these recombination events on viral RNA evolution is profound, as they cause rapid changes within viral genomes. Therefore, in addition to molecular characterization of the new HCRSV isolates, recombination events between *p38* genes of different HCRSV isolates and the effects of such recombination events on the structures of the respective proteins were investigated in this study.

Materials and Methods

The plant samples

During 2019-2020, several *H. rosa-sinensis* plants were observed in Ahvaz and Molasani, Khuzestan province, with ringspot and mottling on their leaves. Leaf samples were collected and taken to the Plant Virology Laboratory of Shahid Chamran University in Ahvaz. The samples were frozen in liquid nitrogen and stored at -80 °C until used for molecular detection studies.

RT-PCR and sequencing

According to the manufacturer's recommendations, total RNA was extracted from symptomatic and asymptomatic leaves using a commercial RNA isolation kit (DENAzist, Iran). To detect the HCRSV genome in the collected samples, a degenerate primer pair Hb-F/Hb-R (Pourrahim *et al., 2*013) was used in RT-PCR to amplify the complete sequence of the CP. RT-PCR products were loaded onto a 1% agarose gel, and the gel was run at 100 V, stained with Safe Satin, and visualized under UV light. The expected amplicons from HCRSV-positive samples were sequenced in both directions (Codon Genetic company, Iran).

Sequence analysis

The edited CP sequences of the isolates studied were generated using BioEdit v. 7.0.9.0 (Hall, 1999) and DNA Baser Sequence Assembler v4 (2013, Heracle BioSoft, www.DnaBaser.com). Phylogenetic analyses of HCRSV isolates were performed using available *p38* sequences from other isolates in the world (Table 1). Sequence alignment was generated using Clustal W in

[DOR: 20.1001.1.22519041.2023.12.1.1.9]

BioEdit v. 7.0.9.0. The maximum likelihood (ML) method was performed for *p38* data with raxmlGUI 2.0 beta (Edler *et al., 2*019), using the general time reversible substitution model with a discrete gamma distribution and invariant sites (GTR + G + I), and the rapid bootstrap option with 1000 replications (MLBS). In addition, the *p38* data matrix was analyzed using the Bayesian inference algorithm (BI) with MrBayes v.3.2.6 (Ronquist *et al., 2*012). The best nucleotide substitution model of evolution, estimated by jModelTest 2 (Darriba *et al., 2*012), was GTR + G + I. The BI analysis was performed with two simultaneous runs of 5 M generations, sampling every 1000 generations, discarding 25*%* of the first trees for calculating posterior probability values (BPP) and standard deviation below 0.01. Two divergent HCRSV isolates were used as an outgroup. Intra-host variability of the *CP* sequence of HCRSV isolate from Ahvaz was assessed using a pipeline implemented in Geneious Prime v2019.1 (http://www.geneious.com). The sequence demarcation tool (SDT, version 1.2) was used to calculate the percent identity matrix between the *p38* sequences of the HCRSV isolates.

Recombination detection analysis (RDA)

Alignment of the new full-length *p38* sequence with other full-length *p38* sequences from GenBank was performed (Table 1). The putative parental sequences and recombination breakpoints were predicted using several methods, including RDP, GENECONV, Bootscan, MaxChi, Chimaera, SiScan, and 3Seq implemented in RDP v.5.5 software. Default settings were used for each method (Martin and Rybicki, 2000). Recombination events detected by at least four of the seven algorithms available in the RDP software with robust statistical support were accepted as reliable predictions.

Table 1 HCRSV isolates used in the phylogenetic analysis and their GenBank accession numbers. Generated sequences are indicated in bold.

Geographic origin	Isolation host	Accession number	Reference
Iran-Khuzestan	*Hibiscus rosa-chinensis*	MZ079600.1	Present study
Iran- Khuzestan	*H. rosa-chinensis*	MN908258.1	Present study
Iran- Guilan	*H. rosa-chinensis*	JX865593.1	Pourrahim *et al., 2*013
Israel	*H. rosa-chinensis*	KC876666.1	Luria *et al., 2*013
USA	*H. rosa-chinensis*	MT512573.1	Olmedo-Velarde *et al., 2*021
Singapore	*H. rosa-chinensis*	X86448.2	Huang *et al., 2*000
New Zealand	*H. rosa-chinensis*	EU554660.1	Tang *et al., 2*008
China	*H. rosa-chinensis*	KY933060.1	unpublished
Malaysia	*H. rosa-chinensis*	MN080500	unpublished
Taiwan	*H. rosa-chinensis*	DQ392986.1	unpublished
Turkey	*H. rosa-chinensis*	KY420908.1	Karanfil and Korkmaz 2017
Turkey	*H. rosa-chinensis*	KY420907.1	Karanfil and Korkmaz 2017
Brazil	*H. rosa-chinensis*	MN331522.1	Ramos-Gonzalez *et al., 2*020
Brazil	*H. rosa-chinensis*	MN331519.1	Ramos-Gonzalez *et al., 2*020
Brazil	*H. rosa-chinensis*	MN331518.1	Ramos-Gonzalez *et al., 2*020
Brazil	*H. rosa-chinensis*	MN331517.1	Ramos-Gonzalez *et al., 2*020
Brazil	*H. rosa-chinensis*	MN331520.1	Ramos-Gonzalez *et al., 2*020
Brazil	*H. rosa-chinensis*	MN331516.1	Ramos-Gonzalez *et al., 2*020
Brazil	*H. rosa-chinensis*	MN331515.1	Ramos-Gonzalez *et al., 2*020
Brazil	*H. rosa-chinensis*	MN331523.1	Ramos-Gonzalez *et al., 2*020
Brazil	*H. rosa-chinensis*	MN331524.1	Ramos-Gonzalez *et al., 2*020
Brazil	*H. rosa-chinensis*	MN331525.1	Ramos-Gonzalez *et al., 2*020
Brazil	*H. rosa-chinensis*	MK279671.1	unpublished
Brazil	*H. rosa-chinensis*	MN331514.1	unpublished
Brazil	*H. rosa-chinensis*	MN331513.1	unpublished
Brazil	*H. rosa-chinensis*	MN331526.1	unpublished
Brazil	*H. rosa-chinensis*	MN331521.1	unpublished

[DOR: 20.1001.1.22519041.2023.12.1.1.9]

Homology modeling of the coat protein of HCRSV isolates

Iterative Threading ASSEmbly Refinement Server (I-TASSER) was used to predict the structural models of parental and recombinant CP sequences (Yang and Zhang, *2*015). The quality of the structures was checked by their C-score, TM-score, and RMSD. Moreover, the reliability of the predicted models of coat proteins from the respective HCRSV isolates was assessed using the Ramachandran plot, Verify-3D score, WHAT-IF packing quality scores (https://servicesn .mbi.ucla.edu/SAVES/), and PROSA energy/Z-score (https://prosa.services.came.sbg.ac.at/prosa. php). PROCHECK compares the geometry of the residues in the models with stereochemical parameters derived from the high-resolution X-ray structures by Ramachandran plot analysis. ERRAT analyzes the statistics of atomic contacts between different atom types (nitrogen, carbon, and oxygen), which is used to distinguish between correctly and incorrectly determined regions of protein structures. A score greater than 50 is usually acceptable and consistent with a high-quality model (Colovos and Yeates, 1993). In the PROSA web tool, the Z-score of a protein is determined as the deviation of the total energy between the native folding of the structure and the energy distribution resulting from random conformations (Al-Khayyat and Al-Dabbagh, 2016). A Z-score outside a range characteristic of native proteins of similar size indicates erroneous structures (Al-Khayyat and Al-Dabbagh, 2016). Finally, the packing quality of the residues of the predicted structure was examined using the WHAT-IF Server, and the model was considered reliable if all residues had a value of WHAT-IF packing quality score above -5 (Jain *et al., 2*014). The structural similarity between the tertiary structures of selected proteins was assessed using the CHIMERA software (ver.1.14.).

Results

Molecular detection of new HCRSV isolates in Iran

Leaf samples of *H. rosa-sinensis* plants showing chlorotic ring spots and mottling symptoms (Fig. 1A) were collected from Ahvaz and Molasani in Khuzestan province. Electrophoresis of RT-PCR products using total RNA from these symptomatic samples confirmed amplification of the expected ~1300 bp fragment (Fig. 1B). The amplified fragments from Ahvaz and Molasani isolates were subjected to sequence in both directions. Edition and assembly yielded 1038 bp and 932 bp contigs that matched the complete and partial sequences of *CP* (*p38*) gene, respectively. The newly assembled sequences of *p38* from Ahvaz (Accession No. MZ079600) and Molasani (Accession No. MN908258) were deposited in the GenBank and compared with those of known isolates by BLAST (nBLAST algorithm). The nBLAST analysis revealed that the *p38* sequence of Ahvaz isolates had the highest pairwise nucleotide identity, 96.34%, with the complete genome of MK279671 accession number (Americas) and had 96.15% pairwise identity with the complete sequence of *p38* of the other Iranian HCRSV isolate (JX865593). The lowest nucleotide identity between the *p38* sequence of the Ahvaz isolate and other complete and partial sequences of *p38* in the GenBank database, 91.52%, was found for the Taiwan isolate (DQ392986). Another sequence obtained in this study, MN908258, showed the highest pairwise identity with an isolate from Ahvaz (MZ079600, 98.50%) and Guilan (JX865593, 96.57%). Molasani and Taiwan isolate also had the lowest nucleotide identity (91.52%), indicating that the Taiwan isolate has a more divergent sequence compared to other HCRSV genomes.

A comparison of the full-length sequence of *p38* of the isolate from Ahvaz with previously known isolates in the GenBank revealed 31 mutations at 31 polymorphic sites (SNPs). The percent identity matrix between the *p38* sequences of the HCRSV isolates was calculated using standard procedures with SDT software (Fig. 1C). The isolate from Taiwan showed again the most divergence from other isolates, including two newly described Iranian isolates, accession No. MZ079600 and MN908258, confirming that their sequence differs from those of other HCRSV genomes.

[DOR: 20.1001.1.22519041.2023.12.1.1.9]

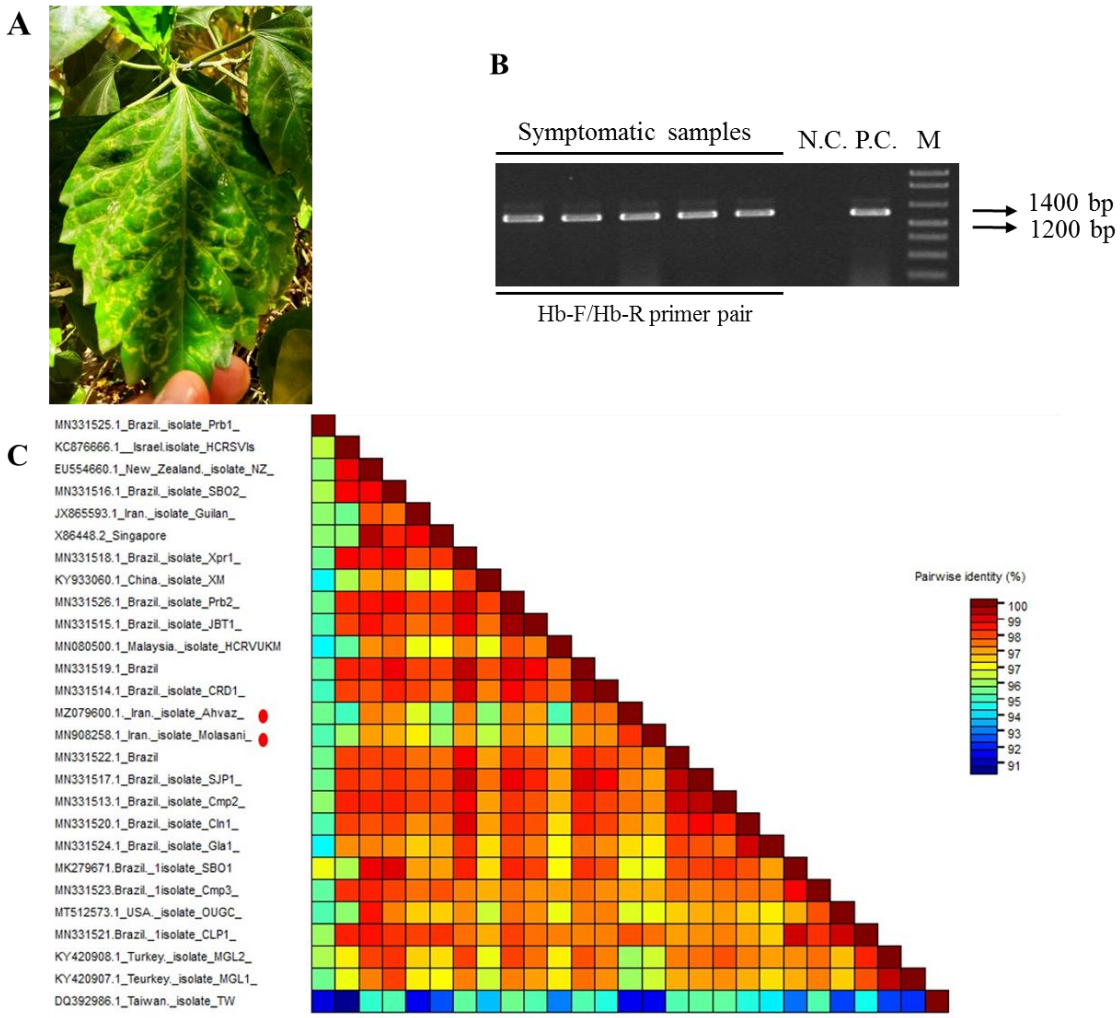

Figure 1 Symptomatic leaf sample from hibiscus plants. Infected plants show chlorotic ring spot patterns on their leaves **(A**). **B.** Electrophoresis patterns of RT-PCR products showed amplified genomic fragments of HCRSV in extracted total RNA from symptomatic plants**. C.** The *p38* sequences were aligned using MUSCLW integrated with SDT, and the percent identity matrix was calculated according to standard procedures. Red circles indicate the isolates obtained in this study. **N. C.**: Extracted total RNA from asymptomatic hibiscus plants was used as a negative control. **P. C.**: Positive control. **M**: 100bp plus DNA ladder RTU (CinaGen, Iran).

Molecular phylogeny; different ancestors for Iranian isolates of HCRSV

The multiple alignments of the *p38* sequences of all 27 HCRSV isolates were used to construct a phylogenetic tree. The tree was rooted in two divergent HCRSV isolates (from China and Taiwan), as these differed most from other HCRSV sequences (Pourrahim *et al.*, 2013). In the phylogenetic tree (Fig. 2), these mostly unrelated isolates are grouped basally to other HCRSV isolates. All other HCRSV isolates were grouped into 12 moderately-supported lineages, including group 1 (MLBS 64%, BPP 0.99), group 2 (MLBS 78%, BPP 0.97), group 3 (MLBS 51%, BPP X.00), group 4 (MLBS 90%, BPP 0.99) and group 10 isolates from Brazil, group 5 isolates under study from Iran (MLBS 100%, BPP 0.1), group 6 isolates from Turkey (MLBS 99%, BPP 0.1), group 7 isolate from Malaysia, group 8 isolates from Brazil and USA (MLBS 79%, BPP 0.1), group 9 isolates from Iran, New Zealand and Singapore (MLBS 55%, BPP 0.85), group 10 isolates from Brazil,

[DOR: 20.1001.1.22519041.2023.12.1.1.9]

group 11 isolate from Israel and group 12 isolate from Brazil. In the phylogenetic analysis based on the *p38* gene, the newly characterized isolates from Khuzestan province were distinct from other HCRSV populations and formed a monophyletic well-supported clade (MLBS 100%, BPP 0.1). The phylogenetic tree also showed a longer evolutionary time for the Brazilian isolate (MN331525) than the other HCRSV isolates based on the partial *CP* gene. The clades didn't show geographic patterns as isolates from different regions clustered in the same clade (Fig. 2).

High rate of recombination between *p38* sequence of HCRSV isolates

To further evaluate the putative recombination events within the entire length of *p38*, we performed recombination detection analysis using the RDP5 software, which contains several recombination detection algorithms, including RDP, GENECONV, BOOTSCAN, MaxChi, Chimaera, SiScan, and 3Seq. Using these seven algorithms, we detected nine acceptable putative recombination events (Table 2). BOOTSCAN, MaxChi, and SiScan predicted three events, while GENECONV did not detect any. The Israeli isolate (KC876666) was predicted to be a potential recombinant by at least five algorithms. In addition, the Ahvaz isolate was also presented as a potential recombinant predicted by BOOTSCAN, MaxChi, Chimaera, and 3Seq algorithms. Interestingly, the isolate from Guilan was identified as the major or minor parent for the potential recombinant isolate from Ahvaz in different algorithms, while the other parent was not identified (Table 2).

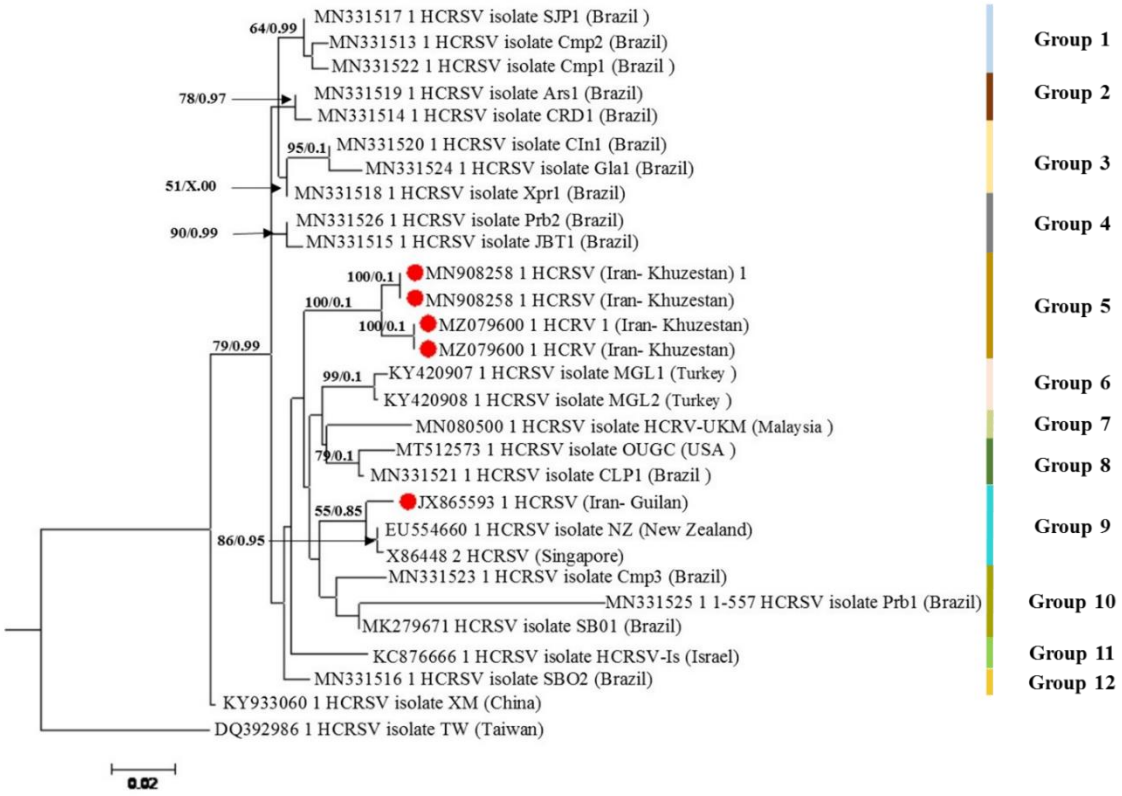

Figure 2 The phylogenetic tree of HCRSV isolates was derived from maximum likelihood analysis based on the sequence of the coat protein gene. The tree was rooted with two HCRSV isolates (XM and TW). Bootstrap values obtained from maximum likelihood analysis, which are at least 50%, and Bayesian posterior probability values (BYPP), which are at least 0.7, are indicated on each branch. The origin of each isolate is indicated in braces. Red circles indicate isolates obtained in this study and other Iranian isolates.

[DOR: 20.1001.1.22519041.2023.12.1.1.9]

Table 2 Summary of unique recombination events identified by the Recombination Detection Program v.5 (RDP5).

Recombinant sequences	Parental sequence (s)		Breakpoints position without gaps		The score for the seven detection methods in RDP4						
	Major	Minor	Begin	End	RDP	GENECONV	BOOTSCAN	MaxChi	Chimaera	SiScan	3Seq
KC876666.1	KY933060.1	MZ079600.1	405	729	1.924E-02	-	-	-	4.023E-02	-	1.420E-02
KC876666.1	MT512573.1	Unknown	992	116	-	-	3.124E-02	1.660E-02	4.088E-02	3.422E-02	4.359E-02
KC876666.1	MZ079600.1	KY933060.1	894	134	-	-	2.195E-03	2.851 E-05	1.180E-02	-	5.667E-03
KC876666.1	MT512573.1	Unknown	815	116	-	-	3.608E-04	1.189E-04	3.315E-04	7.681E-03	-
KC876666.1	Unknown	MT512573.1	116	992	-	-	-	6.410E-04	-	1.021E-15	2.238E-03
MZ079600.1	Unknown	JX865593.1	1008	604	-	-	3.124E-02	1.660 E-02	4.088E-02	3.422E-04	4.359E-02
MZ079600.1	Unknown	JX865593.1	1008	604	-	-	3.124E-02	4.876E-03	4.088E-02	3.422E-04	4.359E-02
MZ079600.1	JX865593.1	Unknown	604	1008	-	-	-	4.876E-03	9.035E-04	3.422E-04	-
MZ079600.1	Unknown	JX865593.1	1008	604	-	-	3.124E-02	1.660 E-02	4.088E-02	3.422E-04	2.563E-02

HCRSV coat proteins are *in vitro* stable with high random coil content

To better understand the molecular aspects of the recombinant CPs of HCRSV isolates, we addressed the relatively poorly described biochemical properties of the p38 proteins. The amino acid sequences and secondary structures of four isolates, including Ahvaz (Iran), Guilan (Iran), Israel, and the USA, which are most involved in recombination events, were analyzed (all comparisons are listed in Table 3). The full-length sequences of all isolates consisted of a 1038 bp fragment encoding 345 amino acids. The molecular weight (Mw) of all isolates was estimated to be~ 37 kDa with theoretical isoelectric point (pI) values close to 9 (Table 3). The number of positively charged residues was greater than that of negatively charged residues in all four predicted structures. Significantly, the instability index was 26.92, 26.92, 24.35, and 26.19 for the Ahvaz, Guilan, Israel, and USA isolates, respectively, suggesting in vitro stability of the encoded proteins. Data obtained from amino acid sequence alignment in the UniProt database showed that the expected HCRSV isolates had a maximum similarity of 97.97% and an identity of 97.39% with each other. The secondary structure analysis of p38 proteins from the expected HCRSV isolates using the SOPMA software revealed these proteins contain predominantly random coils (54.49%, 51.59%, 52.75%, and 47.54% for the isolates from Khuzestan, Guilan, Israel and USA, respectively), followed by alpha helix and β turn (Table 3). According to these results, the p38 proteins of HCRSV isolates have conserved primary and secondary structures. Therefore, their predicted tertiary structures were further investigated to evaluate the effects of recombination on their functional protein structures.

Low sequence to tertiary structure identity between p38 proteins

The tertiary structures of CPs of selected HCRSV isolates were predicted using I-TASSER (Fig. 3). The best models for CPs were further selected based on the indexes listed in Table 4, including RMSD, TM-score, C-score, PROCHECK, ERRAT, and VERIFY_3D scores.

Our results confirmed that the predicted models were reliable. Here, the model with a lower RMSD and TM-score and a higher negative value of the C-score was considered reliable. VERIFY_3D showed that 85.22%, 80.58%, 88.89%, and 72.46% of the residues of the CP models in the isolates from Ahvaz, Guilan, Israel, and USA, had a score between 0.2 and 0.71, which is an acceptable score for the residues. The ERRAT scores were 72.10%, 76.11%, 77.74%, and 67.65/% for the isolates from Ahvaz, Guilan, Israel, and the USA, respectively (Table 4), indicating that the overall quality of nonbonded interactions in the protein structures was appropriate. Finally, the packing quality of each residue by WHAT-IF showed that all scores for each residue were above zero.

[DOR: 20.1001.1.22519041.2023.12.1.1.9]

Table 3 Sequence analysis of the coat proteins of HCRSV isolates from Khuzestan (MZ079600.1), Guilan (JX865593), Israel (KC876666), and USA (MT512573) using the ProtParam server. A comparison of secondary structure content and transmembrane segments was determined with the SOPMA software.

Tools	Parameters	MZ079600.1	JX865593.1	KC876666.1	MT512573.1
ProtParam	Number of amino acids (aa)	345	345	345	345
	Molecular weight (Mw) (Da)	36843.71	36838.74	36912.02	36970.84
	Theoretical isoelectric point (pI)	8.72	8.88	8.87	8.72
	Total number of negatively charged residues (Asp + Glu)	29	29	28	30
	Total number of positively charged residues (Arg + Lys)	33	34	33	34
	Instability index	26.92	26.92	24.35	26.19
	Aliphatic index	81.13	80.87	81.65	81.13
	GRAVY[a]	-0.105	-0.114	-0.020	-0.128
SOPMA	Alpha helix (%)	17.68	22.61	16.81	21.45
	Extended strand (%)	24.35	24.06	26.67	27.54
	Beta turn (%)	3.48	1.74	3.77	3.48
	Random coil (%)	54.49	51.59	52.75	47.54

[a] Grand Average of Hydropathicity index.

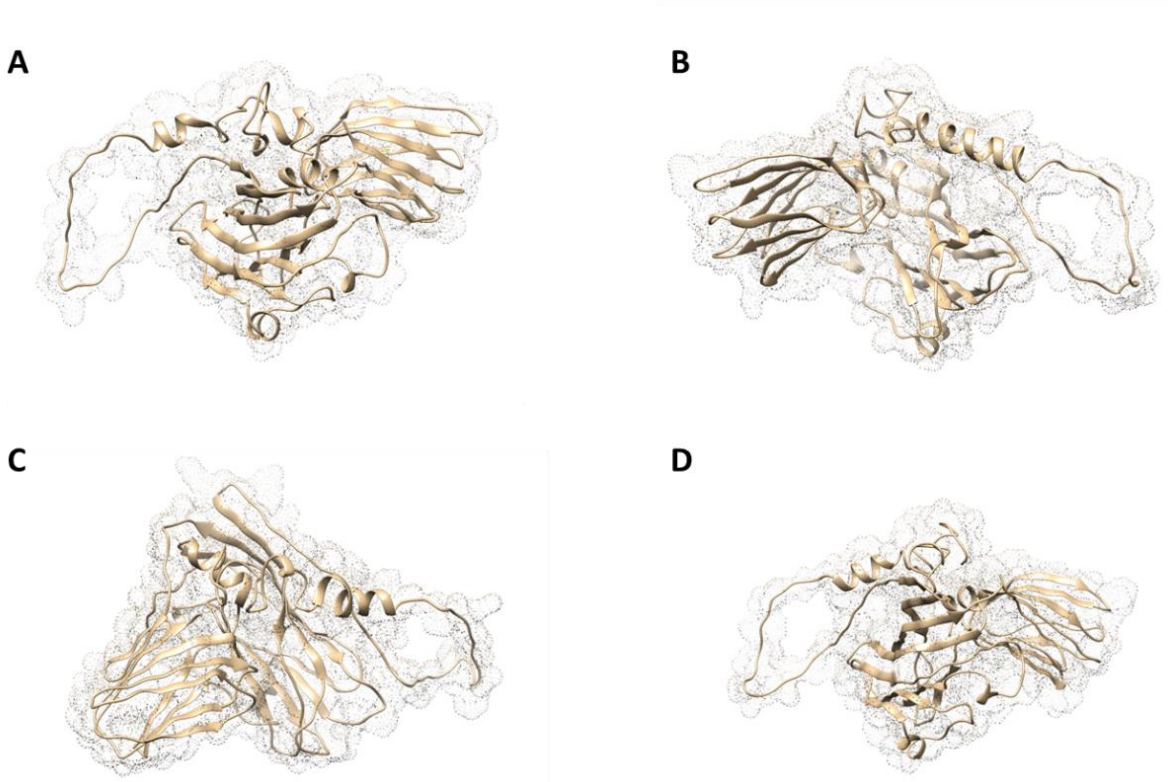

Figure 3 Ribbon representation of the structural models of the coat proteins of isolates from Ahvaz (Iran) (**A**), Guilan (Iran) (**B**), Israel (**C**), and USA (**D**).

[DOR: 20.1001.1.22519041.2023.12.1.1.9]

Table 4 The quality scores for predicted models of coat proteins of HCRSV isolates from Ahvaz, Guilan, Israel, and USA using quality control software.

Isolates	RMSD	TM-score	C-score	Procheck	ERRAT	Verify-3D
MZ079600.1	9.4 ± 4.6	0.56 ± 0.15	-1.27	79.10	72.10	85.22
JX865593.1	8.5 ± 4.5	0.60 ± 0.14	-0.90	81.00	76.11	80.58
KC876666.1	10.6 ± 4.6	0.50 ± 0.15	-1.77	73.90	77.74	88.89
MT512573.1	10.6 ± 4.6	0.50 ± 0.15	-1.76	79.3	67.65	72.46

Despite the high similarity of the primary and secondary structures, the root mean square deviation-RMSD indicates a low structural identity between the p38 proteins involved in recombination events. This low sequence to structure identity between p38 proteins, 8.5 to 10.6 Å, is possible evidence for the effectiveness of detected recombination events at differentiating the CPs of HCRSV isolates.

Discussion

Shrubs of the genus *Hibiscus*, family *Malvaceae*, such as *H. rosa-sinensis* L., *H. cannabinus* L., *H. sabdariffa* L., and *H. trionum* L., are native to tropical and subtropical areas of the world. They are commonly used as ornamental plants in hedgerows and containers, as fibers sources for pulp and cordage production, and as medicinal plants to treat human diseases (da Silva *et al.*, *2*014; Liu and Huang, 2016; Ayadi *et al.*, *2*016; Liang *et al.*, *2*017). *H. rosa-sinensis* grows as an ornamental plant in humid regions of Iran, especially in Khuzestan province. On the leaves of hibiscus plants in Khuzestan province, yellow ring spots and mottling are common symptoms. Following the symptomatology (Pourrahim *et al.*, *2*013), we investigated the occurrence of HCRSV in Khuzestan province by RT-PCR, which led to amplifying the CP gene of new HCRSV isolates. Phylogenetic relationships revealed different ancestors for Iranian isolates from Khuzestan and Guilan provinces. Isolates from other geographic regions are grouped in the same clades, suggesting no geographic separation between different HCRSV populations (Lian *et al.*, *2*013).

Recombination is a pervasive process generating diversity in most viruses. It joins variants that arise independently within the same molecule, creating new opportunities for viruses to overcome selective pressures and adapt to various environments and hosts (Perez-Losada *et al.*, *2*015). During betacaromovirus replication, RNA recombination frequently occurs as the RNA-dependent RNA polymerase changes templates (Cheng and Nagy, 2003). Analysis of recombination between HCRSV isolates revealed frequent recombination events at the 3′ end of *p38* sequences suggesting the presence of recombination signals in this region of the CP gene. RNA recombination has been found to mediate the rearrangement of viral genes, repair deleterious mutations, and acquisition of no-self sequences that affect the phylogeny of viral taxa (Sztuba-Solinska *et al.*, *2*011). Therefore, structural models of the expected proteins were predicted to determine the potential impact of these recombination patterns on the structure of CPs of HCRSV isolates and their likely biological effects.

In addition to structural functions, the CPs of HCRSV also play nonstructural roles in the suppression of gene silencing (Meng *et al.*, *2*008) and interaction with host proteins (Zhang and Wong, 2009). The CP of HCRSV is a major factor in the movement of the virus within host tissues (Niu *et al.*, *2*014). In many RNA plant viruses such as alfamoviruses (Spitsin *et al.*, 1999), cucumoviruses (Suzuki *et al.*, 1991), dianthoviruses (Vaewhongs *et al.*, 1995), sobemoviruses (Brugidou *et al.*, 1995) and tobamoviruses (Fuentes and Hamilton, 1993), the functional CP to form a stable virion is essential for long-distance movement within the host. Overall, these findings demonstrate the important role of the HCRSV CP during the virus infection cycle. Therefore, recombination within the CP-coding sequence would have differential effects on the fitness of new

[DOR: 20.1001.1.22519041.2023.12.1.1.9]

recombinants. Despite the high similarity of amino acid sequences and secondary structures between the recombinant isolates and their minor/major parents (Table 3), the tertiary structures had low structural identity based on root mean square deviation-RMSD (Table 4). These results indicate the likely effects of recombination events on protein structures in different geographic regions.

In summary, we report the occurrence of the first HCRSV isolates from Khuzestan province, indicating the widespread distribution of this species in Iran. Studying the full genome of HCRSV in different parts of the country would clarify the origin of isolates and the genetic structure of the populations. Similar to phylogenetic analyses, the prediction of coat protein structures revealed different probable properties for p38 conserved proteins, which may have resulted from the high rate of recombination events.

Conflicts of interest

The authors declare that they have no conflict of interest.

Author contributions

Saeid Tabein and Seyed Ali Hemmati conceived and designed the experiments; experiments were performed by Nadia Mosharaf, and Saeid Tabein; Saeid Tabein, Seyed Ali Hemmati, and Mehdi Mehrabi-Koushki analyzed the data, and all of the authors wrote the paper. All authors have read and approved the final manuscript.

Acknowledgment

This study was supported by Shahid Chamran University of Ahvaz, Ahvaz, Iran (Grant No.SCU.AP1400.38686).

References

Adams, M. J., Lefkowitz, E. J., King, A. M. Q., Harrach, B., Harrison, R. L., Knowles, N. J., Kropinski, A. M., Krupovic, M., Kuhn, J. H., Mushegian, A. R., Nibert, M., Sabanadzovic, S., Sanfaçon, H., Siddell, S. G., Simmonds, P., Varsani, A., Zerbini, F. M., Gorbalenya, A. E. and Davison, A. J. 2016. Ratification vote on taxonomic proposals to the international committee on taxonomy of viruses. Archives of Virology, 161: 2921-2949.

Adhab, M., Angel, C., Rodriguez, A., Fereidouni, M., Király, L., Scheets, K. and Schoelz, J. E. 2019. Tracing the lineage of two traits associated with the coat protein of the *Tombusviridae*: silencing suppression and HR elicitation in Nicotiana species. Viruses, 11(7): 588.

Al-Khayyat, M. Z. and Al-Dabbagh, A. G. 2016. In silico prediction and docking of tertiary structure of *LuxI*, an inducer synthase of *Vibrio fischeri*. Reports of Biochemistry and Molecular Biology, 4(2): 66-75.

Ayadi, R., Hanana, M., Mzid, R., Hamrouni, L., Khouja, M. L. and Salhi-Hanachi, A. 2016. *Hibiscus Cannabinus* L. «Kenaf»: a review paper. Journal of Natural Fibers, 14(4): 1-19.

Brugidou, C., Holt, C., Yassi, M. N., Zhang, S., Beachy, R. and Fauquet, C. 1995. Synthesis of an infectious full-length cDNA clone of rice yellow mottle virus and mutagenesis of the coat protein. Virology, 206(1): 108-115.

Brunt, A. A. and Spence, N. J. 2000. The natural occurrence of Hibiscus chlorotic ringspot virus (*Carmovirus*; *Tombusviridae*) in aibika or bele (*Abelmoschus manihot*) in some South Pacific Island countries. Plant Pathology, 49(6): 798-798.

Cheng, C. P. and Nagy, P. D. 2003. Mechanism of RNA recombination in carmo-and tombusviruses: evidence for template switching by the RNA-dependent RNA polymerase in vitro. Journal of Virology, 77(22): 12033-12047.

Colovos, C. and Yeates, T. O. 1993. Verification of protein structures: patterns of nonbonded atomic interactions. Protein Science, 2(9): 1511-1519.

da Silva, A. B., Wiest, J. M., Paim, M. P. and Girolometto, G. 2014. Caracterização antibacteriana e fitoquímica de flores de *Hibiscus rosa-sinensis* L. (mimo-de-vênus) e *Hibiscus syriacus* L. (hibisco-da-síria). Revista do Instituto Adolfo Lutz, 73: 264-271.

[DOR: 20.1001.1.22519041.2023.12.1.1.9]

Darriba, D., Taboada, G. L., Doallo, R. and Posada, D. 2012. jModelTest 2: more models, new heuristics and parallel computing. Nature Methods, 9: 772.

Edler, D., Klein, J., Antonelli, A. and Silvestro, D. 2020. raxmlGUI 2.0 beta: A graphical interface and toolkit for phylogenetic analyses using RAxML. Methods in Ecology and Evolution, 12(2): 1-5.

Fuentes, A. L. and Hamilton, R. I. 1993. Failure of long-distance movement of southern bean mosaic virus in a resistant host is correlated with lack of normal virion formation. Journal of General Virology, 74(9): 1903-1910.

Hall, T. 1999. BioEdit: a user-friendly biological sequence alignment editor and analysis program for Windows 95/98/NT. Nucleic Acids Symposium, 41: 95-98.

Huang, M., Koh, D. C, Weng, L. J., Chang, M. L., Yap, Y. K., Zhang, L. and Wong, S. M. 2000. Complete nucleotide sequence and genome organization of hibiscus chlorotic ringspot virus, a new member of the genus Carmovirus: evidence for the presence and expression of two novel open reading frames. Journal of Virology, 74(7): 3149-3155.

Iki, T., Tschopp, M. A. and Voinnet, O. 2017. Biochemical and genetic functional dissection of the P38 viral suppressor of RNA silencing. RNA, 23(5): 639-654.

Jain, R. K., Smith, K. M., Culligan, P. J. and Taylor, J. E. 2014. Forecasting energy consumption of multi-family residential buildings using support vector regression: Investigating the impact of temporal and spatial monitoring granularity on performance accuracy. Applied Energy, 123: 168-178.

Jones, D. R. and Behncken, G. M. 1980. Hibiscus chlorotic ringspot, a widespread virus disease in the ornamental *Hibiscus rosa-sinensis*. Australasian Plant Pathology, 9: 4-5.

Karanfil, A. and Korkmaz, S. 2017. First report of Hibiscus chlorotic ringspot virus in Turkey. New Disease Reports 35: 22.

Lian, S., Lee, J. S., Cho, W. K., Yu, J., Kim, M. K., Choi, H. S. and Kim, K. H. 2013. Phylogenetic and recombination analysis of tomato spotted wilt virus. PloS one, 8: 63380.

Liang, C., Pan, H., Li, H., Zhao, Y. and Feng, Y. 2017. In vitro anticancer activity and cytotoxicity screening of phytochemical extracts from selected traditional Chinese medicinal plants. Journal of the Balkan Union of Oncology, 22(2): 543-551.

Liu, C. and Huang, Y. 2016. Chinese herbal medicine on cardiovascular diseases and the mechanisms of action. Frontiers in Pharmacology, 7: 469.

Luria, N., Reingold, V., Lachman, O. and Dombrovsky, A. 2013. Full-genome sequence of hibiscus chlorotic ringspot virus from Israel. Genome Announcements, 1(6): e01050-13.

Martin, D. and Rybicki, E. 2000. RDP: detection of recombination amongst aligned sequences. Bioinformatics, 16(6): 562-563.

Meng, C., Chen, J., Ding, S. W., Peng, J. and Wong, S. M. 2008. Hibiscus chlorotic ringspot virus coat protein inhibits trans-acting small interfering RNA biogenesis in Arabidopsis. Journal of General Virology, 89(9): 2349-58.

Meng, C., Chen, J., Peng, J. and Wong, S. M. 2006. Host-induced avirulence of hibiscus chlorotic ringspot virus mutants correlates with reduced gene-silencing suppression activity. Journal of General Virology, 87(2): 451-459.

Navarro, J. A. and Pallás, V. 2017. An update on the intracellular and intercellular trafficking of carmoviruses. Frontiers in Plant Science, 8: 1801.

Niu, S., Gil-Salas, F. M., Tewary, S. K., Samales, A. K., Johnson, J., Swaminathan, K. and Wong, S. M. 2014. Hibiscus chlorotic ringspot virus coat protein is essential for cell-to-cell and long-distance movement but not for viral RNA replication. PloS one, 9(11): 113347.

Olmedo-Velarde, A., Hu, J. and Melzer, M. J. 2021. A virus infecting *Hibiscus rosa-sinensis* represents an evolutionary link between cileviruses and higreviruses. Frontiers in Microbiology, 12: 660237.

Pérez-Losada, M., Arenas, M., Galán, J. C., Palero, F. and González-Candelas, F. 2015. Recombination in viruses: mechanisms, methods of study, and evolutionary

[DOR: 20.1001.1.22519041.2023.12.1.1.9]

consequences. Infection, Genetics and Evolution, 30: 296-307.

Pourrahim, R., Ghobakhlo, A. and Farzadfar, S. 2013. Biological and molecular detection of Hibiscus chlorotic ringspot virus infecting *Hibiscus rosa-sinensis* in Iran. Phytopathologia Mediterranea, 52(3): 528-531.

Ramos-González, P. L., Santos, G. F., Chabi-Jesus, C., Harakava, R., Kitajima, E. W. and Freitas-Astúa, J. 2020. Passion fruit green spot virus genome harbors a new orphan orf and highlights the flexibility of the 5′-end of the RNA2 segment across cileviruses. Frontiers in Microbiology, 11: 206.

Ronquist, F., Teslenko, M., Van Der Mark, P., Ayres, D. L., Darling, A., Höhna, S., Larget, B., Liu, L., Suchard, M. A. and Huelsenbeck, J. P. 2012. MrBayes 3.2: efficient Bayesian phylogenetic inference and model choice across a large model space. Systemic Biology, 61(3): 539-542.

Spitsin, S., Steplewski, K., Fleysh, N., Belanger, H., Mikheeva, T., Shivprasad, S., Dawson, W., Koprowski, H. and Yusibov, V. 1999. Expression of alfalfa mosaic virus coat protein in tobacco mosaic virus (TMV) deficient in the production of its native coat protein supports long-distance movement of a chimeric TMV. Proceedings of the National Academy of Sciences of the United States of America, 96(5): 2549-2553.

Suzuki, M., Kuwata, S., Kataoka, J., Masuta, C., Nitta, N. and Takanami, Y. 1991. Functional analysis of deletion mutants of cucumber mosaic virus RNA3 using an in vitro transcription system. Virology, 183(1): 106-113.

Sztuba-Solińska, J., Urbanowicz, A., Figlerowicz, M. and Bujarski, J. J. 2011. RNA-RNA recombination in plant virus replication and evolution. Annual Review of Phytopathology, 49: 415-443.

Tang, J., Elliott, D. R., Quinn, B. D., Clover, G. R. G. and Alexander, B. J. R. 2008. Occurrence of Hibiscus chlorotic ringspot virus in *Hibiscus* spp. in New Zealand. Plant Disease, 92(9): 1367-1367.

Vaewhongs, A. A. and Lommel, S. A. 1995. Virion formation is required for the long-distance movement of red clover necrotic mosaic virus in movement protein transgenic plants. Virology, 212(2): 607-613.

Waterworth, H. E., Lawson, R. H. and Monroe, R. L. 1976. Purification and properties of Hibiscus chlorotic ringspot virus. Phytopathology, 66(5): 570-575.

Yang, J. and Zhang, Y. 2015. Protein structure and function prediction using I-TASSER. Current Protocols in Bioinformatics, 52: 5-8.

Zhang, X. and Wong, S. M. 2009. Hibiscus chlorotic ringspot virus upregulates plant sulfite oxidase transcripts and increases sulfate levels in kenaf (*Hibiscus cannabinus* L.). Journal of General Virology, 90(12): 3042-3050.

Zhou, T., Fan, Z., F, Li, H. F. and Wong, S. M. 2006. Hibiscus chlorotic ringspot virus p27 and its isoforms affect symptom expression and potentiate virus movement in kenaf (*Hibiscus cannabinus* L.). Molecular Plant Microbe Interaction, 19(9): 948-957.

[DOR: 20.1001.1.22519041.2023.12.1.1.9]

آنالیز مولکولی و درون‌رایانه‌ای پروتئین پوششی جدایه‌های ویروس لکه حلقوی سبزرد ختمی چینی

نادیا مشرف[1]، سعید تابعین[1*]، مهدی مهرابی کوشکی[1]، سیدعلی همتی[1] و ابوذر قربانی[2]

۱- گروه گیاه‌پزشکی، دانشکده کشاورزی، دانشگاه شهید چمران اهواز، اهواز، ایران.
۲- پژوهشکده کشاورزی هسته‌ای، پژوهشگاه علوم و فنون هسته‌ای، کرج، ایران.
پست الکترونیکي نویسنده مسئول مکاتبه: s.tabein@scu.ac.ir
دریافت: ۱۰ مهر ۱۴۰۱؛ پذیرش: ۹ بهمن ۱۴۰۱

چکیده: ویروس لکه حلقوی سبزرد ختمی چینی، متعلق به جنس *Betacarmovirus* و تیره *Tombusviridae*، بیمارگر رایج گیاهان ختمی در مناطق گرمسیری و نیمه‌گرمسیری محسوب می‌شود. در طی سال‌های ۱۳۹۹-۱۴۰۰، نمونه‌های برگ بوته‌های ختمی چینی، *Hibiscus rosa-sinensis* L.، با علایم پیسک و لکه‌های حلقوی سبزرد از شهرستان‌های اهواز و ملاثانی در استان خوزستان جمع‌آوری شد. آران‌ایِ کل استخراج شده از نمونه‌های دارای علایم، برای تکثیر توالی ژن کدکننده پروتئین پوششی (*p38*) ویروس لکه حلقوی سبزرد ختمی چینی، به‌وسیله واکنش زنجیره‌ای پلی‌مراز همراه با ترانویسی معکوسی مورد ارزیابی قرار گرفت. توالی‌های کامل (۱۰۳۸ جفت باز) و ناقص (۹۳۲ جفت باز) از ژن *p38* به‌ترتیب از جدایه‌های اهواز و ملاثانی به‌دست آمد که در بانک ژن ثبت شدند. توالی‌های به‌دست آمده با توالی‌های مشابه در بانک ژن با استفاده از نرم‌افزار nBLAST و همچنین مطالعات تبارزایی مورد مقایسه قرار گرفت. درخت تبارزایی مبتنی بر توالی‌های *p38* اجداد متفاوتی را برای جدایه‌های ایرانی نشان داد. علاوه‌براین، جدایه‌های مورد بررسی بدون در نظر گرفتن پراکنش جغرافیایی در شاخه‌های درخت تبارزایی طبقه‌بندی شدند که می‌تواند نشان‌دهنده عدم افتراق جمعیت ویروس براساس محل جغرافیایی و نیز ارتباط جمعیت‌های ویروس با یکدیگر باشد. آنالیز نوترکیبی توالی‌های *p38* منجر به تخمین حداقل دو جدایه نوترکیب قابل قبول، اهواز و اسرائیل، شد. تخمین درون‌رایانه‌ای ساختمان پروتئین پوششی جدایه‌های دخیل در وقایع نوترکیبی نشان‌دهنده تشابه پایین این ساختارها در مقایسه با توالی نوکلئوتیدی ژن‌های کدکننده پروتئین پوششی در جدایه‌های ویروس بود. به‌طور کلی، علاوه بر گزارش دو جدایه جدید از ویروس لکه حلقوی سبزرد ختمی چینی از ایران، مطالعه حاضر تمایز ژنتیکی بالایی برای این ویروس از طریق سازوکار نوترکیبی نشان داد و همچنین پیشنهاد می‌دهد که معیارهای طبقه‌بندی این گروه از ویروس‌ها می‌تواند از سطح تشابه پایین توالی نوکلئوتیدی به درصد بالاتر و نیز استفاده از آنالیزهای ساختار پروتئین در این معیارها تغییر کند.

واژگان کلیدی: ویروس لکه حلقوی سبزرد ختمی چینی، پروتئین پوششی، نوترکیبی، ساختار درجه سوم

[DOR: 20.1001.1.22519041.2023.12.1.1.9]